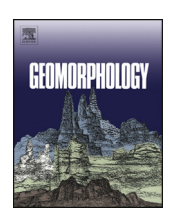


Contents lists available at ScienceDirect

Geomorphology

journal homepage: www.elsevier.com/locate/geomorph



The impact of run-of-river dams on sediment longitudinal connectivity and downstream channel equilibrium



Francis J. Magilligan ^{a,*}, Maura O. Roberts ^b, Mackenzie Marti ^b, Carl E. Renshaw ^b

- ^a Department of Geography, Dartmouth College, Hanover, NH 03755, United States of America
- ^b Department of Earth Sciences, Dartmouth College, Hanover, NH 03755, United States of America

ARTICLE INFO

Article history:
Received 13 August 2020
Received in revised form 4 December 2020
Accepted 8 December 2020
Available online 11 December 2020

Keywords:
Dams
Bedload
Passive tracer
RFID
Connectivity
Virtual velocity

ABSTRACT

Considerable research over the past several decades shows that dams, especially large, flow regulating structures, fragment watersheds and serve to disconnect the normative downstream flux of sediment and nutrients. Less attention has addressed smaller, channel-spanning Run-of-River (RoR) dams that are more commonly distributed throughout watersheds. Taking advantage of a suite of RoR dams in New England (USA), we quantify bedload flux into, through, and beyond the reservoir, and we calculate the residence time of gravel clasts.

We used traditional channel surveys to evaluate (dis)equilibrium channel form and develop two equilibrium metrics based on bankfull shear stress and the bankfull Shields parameter. Additionally, we compartmentalize the bankfull channel Shields parameter as a linear combination of bedload and suspended load components to better quantify channel evolution in response to changes in sediment supply. To accomplish these goals, we embedded Radio Frequency Identification (RFID) PIT tags in 791 gravel clasts ranging in size from 15 mm to 81 mm, which were subsequently deployed within and upstream of the impounded reservoirs. Among the 503 tracers that were transported from their deployment location, the median cumulative distance traveled was 30 m and the maximum cumulative displacement during the study period was 758 m. Of the total tagged rocks placed at all five sites, 276 rocks were displaced over the dam, 204 of which spent time in the reservoir between high discharge events; the rest were transmitted through the reservoir and over the dam in a single high discharge event. Among those tracers that spent time in the reservoir prior to transmission over the dam, the average reservoir residence times at the different sites ranged from 19 to 203 days. The median grain sizes of tracers that were transported over the dam were identical to those that moved during the study period and similar to the median grain size of the channel bed. The distribution of virtual velocities of those tracers that moved was approximately log-normal and very broadly distributed over more than six orders of magnitude. An analysis of variance revealed that the distribution of velocities was partitioned into two statistically similar groups; with slower velocities in the two smaller watersheds (13 km²-21 km²) with higher average slopes compared to the larger watersheds (89 km²-438 km²) with lower average slopes. We conclude that RoR dams transmit and trap the upstream sediment supply within the same range of physical conditions that produce mobility and trapping in the river's natural reach-scale morphological units. Because RoR dams are likely not trapping more sediment than is typically sequestered in natural river reaches, these dams do not disconnect the normative downstream flux of sediment nor result in channel morphological disequilibrium downstream of the dam. Reaches below RoR dams have similar geomorphic properties to comparable equilibrium reaches unaffected by dams. However, the minimal effect that small, channel spanning RoR dams have on the morphological equilibrium state of a channel does not suggest that RoR dams have no ecological footprint.

© 2020 Published by Elsevier B.V.

1. Introduction

By disrupting the downstream flux of sediment and nutrients and blocking the upstream mobility of resident and diadromous fishes (Nilsson et al., 2005; Nilsson and Svedmark, 2002), large dams profoundly affect hydrologic, ecological, and geomorphic systems at local (Brandt, 2000; Church, 1995; Curtis et al., 2010; Gregory and Park,

* Corresponding author. E-mail address: magilligan@dartmouth.edu (F.J. Magilligan). 1974; Juracek, 2000), watershed (Graf, 1999; Magilligan et al., 2008), and global (Syvitski et al., 2005; Vorosmarty et al., 2003) scales. However, in contrast to the considerable research on large, flow regulating dams, less attention has been given to smaller Run-of-River (RoR) dams, notwithstanding their greater occurrence across the landscape. In the United States (US), for example, the National Inventory of Dams (NID) documents >80,000 large dams, while the number of smaller dams may exceed two million (Smith et al., 2002).

Run-of-River dams span the width of the channel but do not impede discharge (Csiki and Rhoads, 2010). They have short hydraulic residence times, with reported values of <2 h (Ashley et al., 2006; Poff and Hart,

2002), and limited sediment trapping efficiency (Brune, 1953), especially at high flows (Csiki and Rhoads, 2014; Pearson et al., 2011). Where some sediment storage occurs, or sediment flux is partially attenuated, the downstream impacts of RoR dams mirror those of larger structures with statistically significant bed grain coarsening (Fencl et al., 2015; Magilligan et al., 2016a) or significant decreases in fine sediment (Csiki and Rhoads, 2010; Skalak et al., 2009). In other cases, RoR dams are not generally observed to create significant discontinuities in channel morphology or sediment character (Csiki and Rhoads, 2014).

The muted downstream impacts of RoR dams are likely caused by their limited sediment trapping efficiency, as evidenced by active scour and fill processes in the reservoir behind RoR dams (Csiki and Rhoads, 2014; Pearson et al., 2011), particularly after the reservoir storage capacity is filled (Major et al., 2012). Pearson et al. (2011) documented that reaches downstream of the RoR Merrimack Village Dam were commonly characterized by episodic deposition and remobilization of material (primarily sand) transported over the dam. Less is known about the transport of coarser material over RoR dams, but Pearson and Pizzuto (2015), based on field observations and 1D flow modeling, hypothesized that sediment deposition in the reservoir constructs a ramp up to the dam crest that facilitates transport of coarse material over the dam. They modeled the potential for coarse sediment transport over an impoundment with a ramp and estimated that clasts up to ~23 mm could move through the reservoir and ultimately over the dam crest. Yet they did not directly observe coarse sediment transport over the impoundment. Casserly et al. (2020), however, recently observed tracer particles greater than the median grain size travelling through and over two low-head dams in southeastern Ireland, and argued that the retention of coarser sediment after reservoir scour events led to transient storage behind the dam and resulted in transient supply-limited conditions downstream.

An important outstanding question is: when sediment flux disruption across RoR dams occurs, is it sufficient to cause channel morphological disequilibrium downstream of the dam? Although significant changes in channel bed grain size are observed downstream of some RoR dams (Csiki and Rhoads, 2010; Fencl et al., 2015; Magilligan et al., 2016a; Skalak et al., 2009), it is unknown if possible covariate adjustments in other channel parameters (i.e., flow depth, slope) are sufficient to compensate for these changes in channel bed grain size such that an equilibrium channel form is maintained even as grain size changes (Curtis et al., 2010; Dade et al., 2011; Renshaw et al., 2019).

Here we focus on the disruption of bedload transport because it is more likely to be affected by RoR dams than suspended sediment transport. To directly link the frequency that bedload sediment is transported over RoR dams with downstream channel (dis)equilibrium, we couple field monitoring of sediment transport over RoR dams using Radio Frequency Identification (RFID) PIT (passive integrated transponders) tags in coarse gravel and cobble clasts with detailed reach scale analyses upstream and downstream of the dams to characterize potential channel adjustments following impoundment. Importantly, the goal herein is as much to evaluate the efficacy of sediment transport across RoR dams as it is to document and quantify the ways in which stream channels might maintain equilibrium conditions relative to transient and/or sustained shifts in sediment supply.

Identifying equilibrium is often difficult in fluvial systems as the signal to noise ratio can be muted by the inherent variability of hydrologic and geomorphic processes. At the extreme end where significant sediment trapping and hydrologic alterations occur at larger, flow-regulating dams, it is easier to identify channel dis-equilibrium following impoundment (Magilligan et al., 2013). However, for RoR dams where streamflow is minimally altered and sediment trapping is similarly less affected, traditional metrics for evaluating geomorphic change, such as channel width or cross-sectional area (Csiki and Rhoads, 2014), may not be sufficiently sensitive to identify geomorphic dis-equilibrium. To enhance the sensitivity of our analyses, we obviate a singular focus on channel parameters by representing the possible

adjustments in terms of the Shields parameter and bed shear stress that simultaneously represent variations in characteristic flow depth, slope, and, in the case of the Shields parameter, grain size, to characterize (dis)equilibrium (Curtis et al., 2010; Dade et al., 2011; Renshaw et al., 2019). Our research questions are: (1) How frequently, if at all, do RoR dams trap bedload sediment; (2) given the frequency of sediment trapping, what is the expected average residence time of sediment within RoR reservoirs; (3) are the downstream channels able to maintain equilibrium vis-à-vis these changes in sediment flux? By taking advantage of the natural experiments provided by RoR dam emplacements that chronically perturb sediment flux in a manner that is fixed in time and space, our research questions seek to improve our understanding of the covariate channel evolution following a disturbance and thereby advance our understanding of the fundamental controls on the equilibrium form of a river channel.

2. Study sites and background

During 2016-2017, we sampled eight dammed sites (Figs. 1 and 2, Table 1) within the Upper Connecticut River watershed, one of the most dammed regions in the US (Graf, 1999; Magilligan et al., 2016b). These dams, ranging in age from 60 to 97 yr old, represent a range of dam heights, slopes, flow regimes, and drainage areas (Table 1). Morphologically, the study reaches are dominated by riffles, pools, and plane bed units (Montgomery and Buffington, 1997). The channel bed surface grain size is predominantly gravel across all study sites, though locally at a few sites there is significant sand content; at 2 of the 69 measured transects the sand content exceeded 50%. The percentage of filled reservoir volume ranges from 27 to 95%. No known recent (last decade) history of dredging exists at any of these sites. Seven of these sites have RoR dams, generally constructed in the twentieth century to provide local water supply. As a point of comparison, one of the dams is a large (>40 m high) flood control, impoundment dam with a permanent reservoir. At all sites we used the bankfull channel Shields parameter to assess the (dis)equilibrium form of the channel above and below the dams. At five of these sites (Fig. 1: Fay Brook Dam (FBR), West Windsor Dam (WIND), Wild Ammonoosuc Dam (WAM), and Charlie Brown Dam (CBR)), we tracked gravel into, within, and beyond the reservoir.

The bedrock geology at all eight sites is primarily composed of Paleozoic-age metamorphic and igneous rocks, which is typical of the region (Nicholson et al., 2006). Because of the resistant nature of the local geology and the presence of coarse-grained Pleistocene glacial deposits, rivers in New England tend to be dominated by coarse sediment, with some of the lowest fine-grained suspended sediment concentrations (less than 200 mg/L) in the country (Rainwater, 1962). Vermont and New Hampshire experience a humid continental climate, with all basins receiving an average annual precipitation between 100 and 115 cm/yr (PRISM Climate Group, 2004). The first season of sampling (2016) was typified by below-normal precipitation and above-normal temperatures combining to generate severe drought conditions throughout New England (NOAA, 2017). River flows rebounded somewhat in 2017 with a wetter spring and a moderate flood (2-5 yr recurrence interval) that occurred throughout the study area in July of 2017.

3. Methods and analytical approaches

3.1. Equilibrium metric

Mackin (1948) first qualitatively linked equilibrium channel form to sediment transport dynamics. To quantify this concept, Dade and Friend (1998) and Dade et al. (2011) noted that conventional sediment transport equations often define sediment flux as a function of the Shields

parameter, θ , a dimensionless ratio of bed shear stress τ to submerged particle weight:

$$\theta = \frac{\tau}{\Delta \rho g d} = \frac{hS}{R d} \tag{1}$$

where $\Delta \rho = \rho_s - \rho_f$, where ρ_s and ρ_f are the solid and fluid densities, g is the gravitational acceleration, d is the characteristic grain size, h is the flow depth, S is the slope, and the relative buoyant density $R = \Delta \rho/\rho_f$. On the right-hand side of this equation the depth-slope product is used to approximate the bed shear stress (Leopold et al., 1964).

Dade and Friend (1998) and Dade et al. (2011) combined conventional expressions for sediment transport as a function of the Shields parameter with a quadratic drag law to determine constraints on values for the bankfull Shields value when the equilibrium channel form is defined, following Mackin (1948), as one in which neither deposition nor erosion occurs. They showed that for bedload-dominated systems under bankfull discharge, the bankfull Shields parameter θ_{bf} is similar to the critical value θ_{cr} required for the onset of significant sediment transport. In bedload-dominated channels at equilibrium, the observed range for θ_{bf} is between 0.03 and 0.09 (Kellerhalls, 1967; Li et al., 2015; Parker, 1978; Parker et al., 2007; Trampush et al., 2014). Roberts et al. (2020) showed that although the onset of sediment motion does not occur at a singular Shields value, θ_{cr} can be defined as that corresponding to a 50% chance of particle movement during a high discharge event. Lamb et al. (2008) empirically observed that θ_{cr} scales with slope as θ_{cr} ~ $S^{0.25}$, with θ_{cr} falling within the observed range of θ_{bf} for bedloaddominated channels for $\sim 0.001 < S < \sim 0.1$. Thus for bedloaddominated systems with moderate slopes, the departure of the bankfull Shields parameter from the typically observed range of critical Shields provides a quantitative metric of channel form disequilibrium (Renshaw et al., 2019).

High sand content above and below some RoR dams permits mixed-load transport, and thus the above analysis for bedload systems does not apply to these cases. Indeed, Dade and Friend (1998) showed that under conditions of mixed-load transport, $\theta_{bf} > \theta_{CP}$. Recently, Dunne and Jerolmack (2020) suggested that river geometry adjusts to the threshold fluid entrainment stress t_{CP} of the most resistant material lining the channel which, following Schumm (1960), they suggest that fine-grained (d < 1 cm) channels may be limited by the entrainment stress of the channel banks.

To capture this transition from a bedload-dominated system where the channel geometry is proposed to be a function of a critical Shields parameter (Dade and Friend, 1998) to fine grained systems where channel geometry is proposed to be a function of a critical shear stress (Dunne and Jerolmack, 2020), we propose that the equilibrium bankfull Shields parameter θ_{bf} is a the linear combination of bedload θ_{bed} and suspended load θ_{ss} components:

$$\theta_{bf} = \theta_{ss} + \theta_{bed} \tag{2}$$

As noted above, for bedload dominated systems $\theta_{bed} = \theta_{cr}$. For suspended load dominated systems we propose:

$$\theta_{ss} = \frac{\tau_{cr}}{\Delta \rho g d} \tag{3}$$

where t_{cr} is the critical shear stress. Defining the transitional grain size d_o as the grain size at which $\theta_{ss} = \theta_{bed}$, then when $d = d_o$:

$$\theta_{ss} = \theta_{bed} = \theta_{cr} = \frac{\tau_{cr}}{\Delta \rho g d_{o}} \tag{4}$$

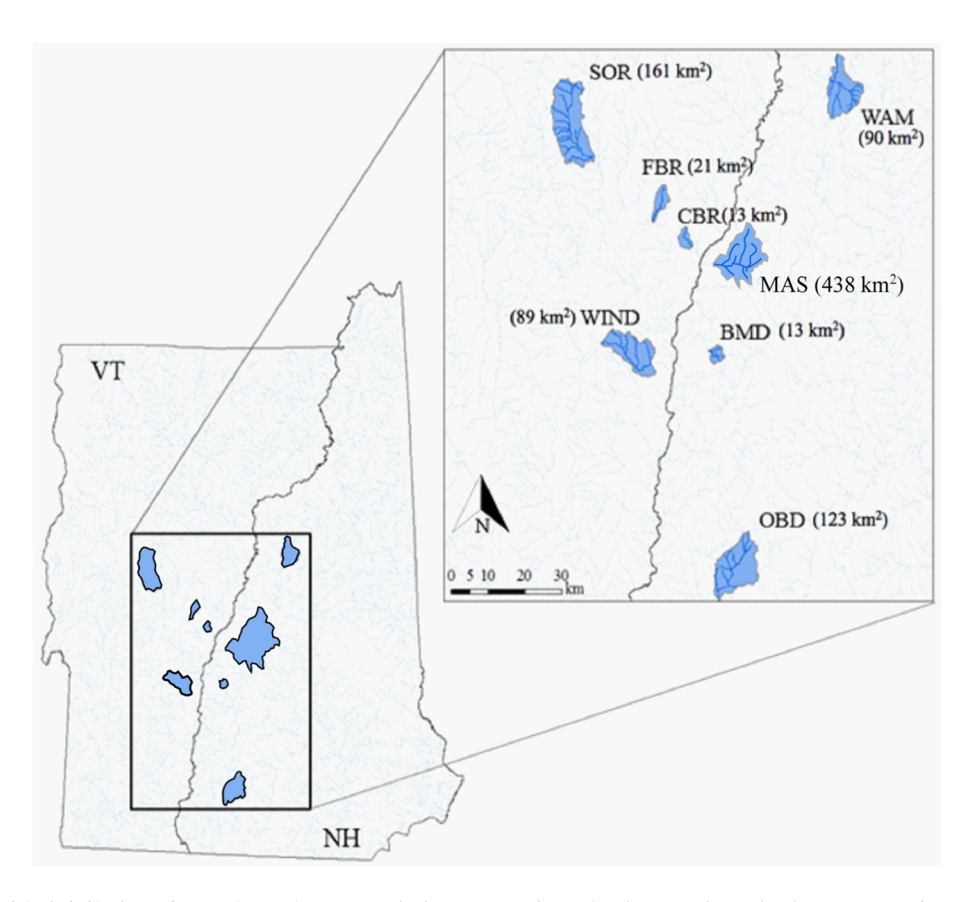


Fig. 1. Locations of watersheds included in the study. Four sites are in Vermont: Charles Brown Brook Dam (CBR), Fay Brook Dam (FBR), Sargent Osgood Roundy Dam (SOR), and Windsor Dam (WIND). Three are in New Hampshire: Blow-Me-Down Brook Dam (BMD), Wild Ammonoosuc River Dam (WAM), and the Otter Brook Dam (OBD). (Color figure available online)

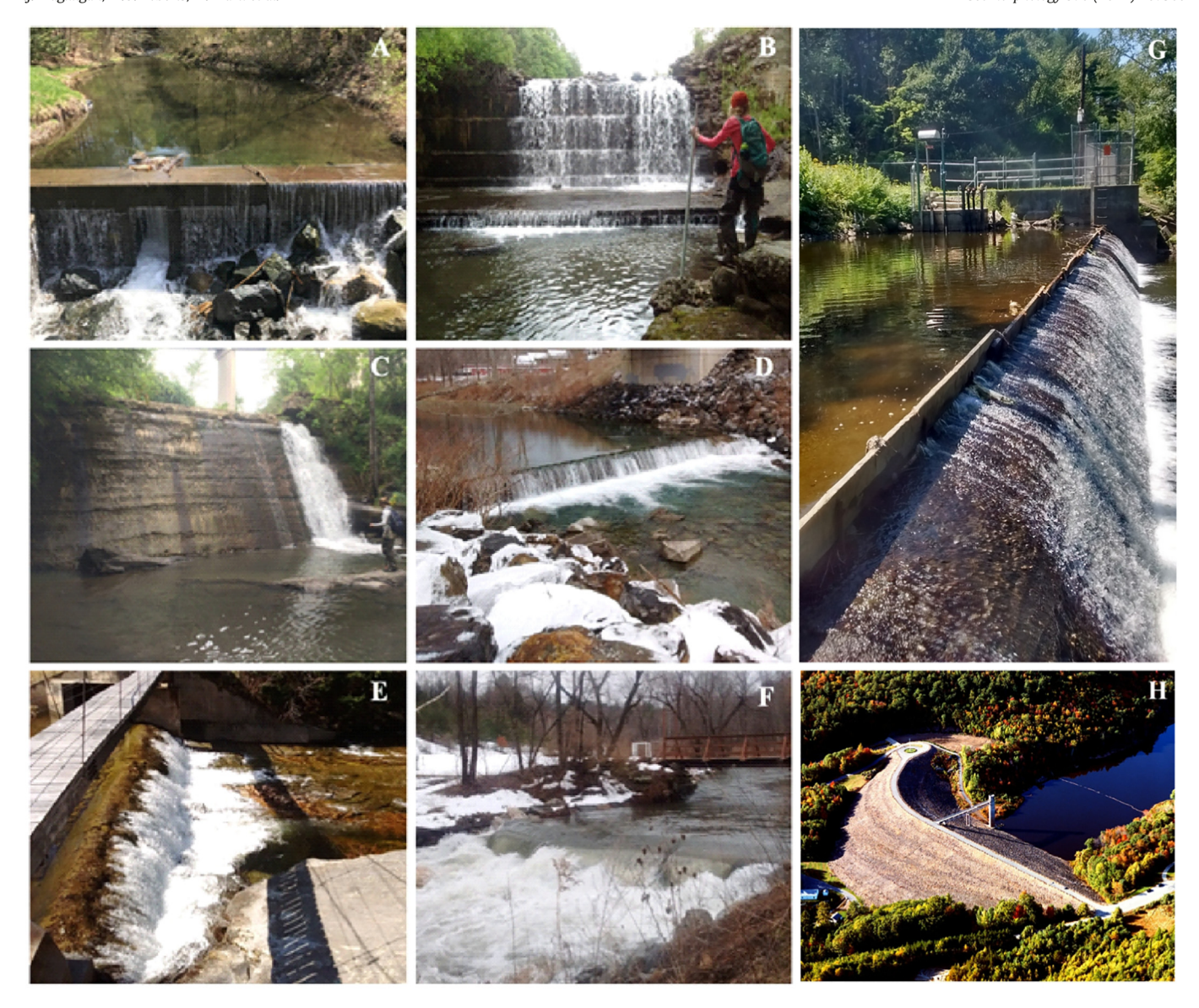


Fig. 2. Photos of sampling sites. (A) Blow Me Down Brook Dam in Cornish, NH (BMD). This is the only dam where discharge flows partially through a top flume. (B) Charles Brown Brook Dam in Norwich, VT (CBR). (C) Fay Brook Dam in Sharon, VT (FBR). (D) Sargent-Osgood Roundy Dam in Randolph, VT (SOR). This dam was removed in Fall 2016. (E) Wild Ammonosuc Dam in Benton, NH (WAM). (F) West Windsor Dam in West Windsor, VT (WIND). This dam was removed in Fall 2017. (G) Mascoma Dam in Lebanon, NH (MAS). (H) Otter Brook Dam in Keene, NH (OBD). Photo courtesy of US Army Corps of Engineers. (Color figure available online)

Table 1Site characteristics. Sites in bold are dams where RFID sampling occurred.

Dam	Dam Style	Drainage Area (km²)	2-yr flow (m ³ /s)	Dam Height (m)	Reservoir Width (m)	Pool Length (m)	Percent Filled	Year bulit	Upstream Slope (%)	Upstream d ₅₀ (mm)	Downstream d ₅₀ (mm)
Blow Me Down Brook Dam (BMD)	Top flume	13	8.8	2.5	11.1	65	73	1934	3.1	68 ± 10	71 ± 20
Charles Brown Brook Dam (CBR)	Flow over	13	6.6	3.6	5.2	82	96	1920	1.2	18 ± 10	13 ± 10
Fay Brook Dam (FBR)	Flow over	21	8.6	5.1	4.8	43	90	Unknown	1.2	21 ± 10	24 ± 10
Mascoma Dam (MAS)	Flow over	438	78.4	1.4	17.5	100	62	1929	1.1	64 ± 15	75 ± 25
Sergeant Osgood-Roundy Dam (SOR)	Flow over	161	61	1.5	20	192	49	1939	0.2	13 ± 10	21 ± 10
West Windsor Dam (WIND)	Flow over	90	36.5	1.5	11.7	70	50	Unknown	0.5	56 ± 20	56 ± 10
Wild Ammonoosuc River Dam (WAM)	Flow over	89	37.9	1.8	17.3	50	49	1927	0.6	33 ± 30	35 ± 20
Otter Brook Dam (OBD)	Impoundment	123	37.7	40.5	205	1600	-	1955	0.8	56 ± 20	72 ± 20

Rearranging:

$$\frac{\tau_{cr}}{\Delta \rho g} = d_o \theta_{cr} \tag{5}$$

and inserting this into the definition of θ_{ss} (Eq. (3)):

$$\theta_{\rm ss} = \left(\frac{1}{d}\right) \frac{\tau_{\rm cr}}{\Delta \rho g} = \left(\frac{1}{d}\right) d_0 \theta_{\rm cr} \tag{6}$$

and thus Eq. (2) can be written:

$$\theta_{bf} = \theta_{ss} + \theta_{bed} = \frac{d_o \theta_{cr}}{d} + \theta_{cr} = \theta_{cr} \left(1 + \frac{d_o}{d} \right)$$
 (7)

In Fig. 3a we fit this model to the distribution of bankfull Shields values compiled by Trampush et al. (2014). The data in Fig. 3 come from streams thought to be in equilibrium with modern conditions, although it is likely that this is not true in all cases. Nonetheless, we take the data in Fig. 3 as representative of the natural variation of channel form for undisturbed systems. In calculating the Shields parameter, we take the median grain size as the characteristic grain size. Our proposed model (Eq. 7) has two free parameters, θ_{cr} and d_o . We used Excel's Solver function to fit Eq. (7) to the Trampush et al. (2014) dataset by minimizing the sum of the squared differences between the log transformed values of the model and observed bankfull Shields. This fitting gives $\theta_{cr} = 0.041 \pm 0.003$ and $d_o = 0.018 \pm 0.003$ m. Using these values in Eq. (5) yields $t_{cr} = 12 \pm 1$ Pa, which is similar to, albeit somewhat higher than, the range of fluid entrainment stresses ($6 \le t_{cr} \le 9$ Pa) measured in the laboratory for sand/kaolinite-clay mixtures meant to represent cohesive riverbanks (Dunne et al., 2019) and directly measured

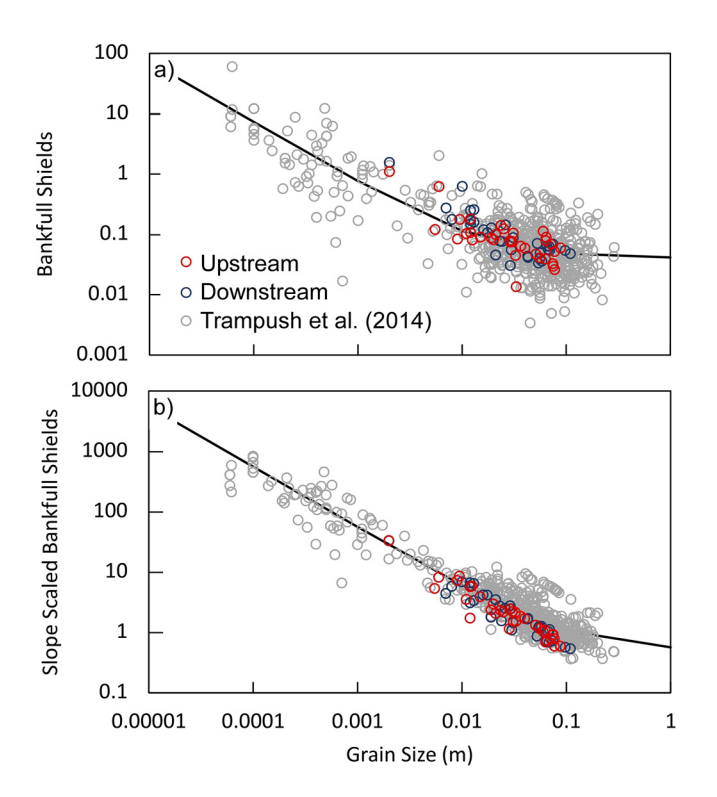


Fig. 3. Bankfull channel Shields parameter (a) and slope-scaled Shields parameter (b) values as a function of grain size. Solid lines are best fit models representing a linear combination of bedload and suspended load components (Eqs. (7) and (10)). Gray circles show the distribution of bankfull Shields and slope-scaled Shields values compiled by Trampush et al. (2014) taken to represent streams in equilibrium with modern conditions. Bankfull Shields and slope-scaled Shields values upstream (red circles) and downstream (blue circles) are indistinguishable from each other and from those of streams in equilibrium.

(4.5 Pa) on the Mullica River (Dunne and Jerolmack, 2020). The uncertainty in the directly measured entrainment stress was not reported by the authors, but we estimate it to be at least \pm ~1 Pa. The higher shear stress from the fit to the bankfull Shields data could reflect the observation that the shear stress experienced by the channel banks is estimated to be about 20% less than the average value estimated from the bankfull dimensions (Parker, 1978).

We can improve the fit of the model by recognizing that slope often covaries with other channel geometric parameters. To account for this, we define a slope-scaled bankfull Shields parameter, T, such that:

$$T = \frac{\theta}{S^{1-\alpha}} = \frac{hS^{\alpha}}{Rd} \tag{8}$$

We recognize that the appropriate slope scaling may differ for bedload and suspended load systems. Although it is possible to use different scaling exponents for each component (bedload and suspended load), we found that the bankfull Shields data are insufficient to adequately constrain the parameters of such a model and thus use the simplified scaling in Eq. (8). As before, we assume that the bankfull geometry is a linear combination of bedload and suspended load components:

$$T_{bf} = T_{bed} + T_{ss} \tag{9}$$

Assuming T_{bed} is equal to a constant T_{cr} and $T_{ss} = \frac{d_0 T_{cr}}{d}$, this can be rewritten as:

$$T_{bf} = T_{cr} \left(1 + \frac{d_o}{d} \right) \tag{10}$$

Fitting this model to the Trampush et al. (2014) dataset yields $T_{cr}=0.51\pm0.11$, $d_o=0.11\pm0.04$ m and $\alpha=0.35\pm0.04$. Recognizing that it follows from Eq. (8) that

$$T_{cr}S^{1-\alpha} = \frac{\tau_{cr}}{\Delta \rho g d} \tag{11}$$

then for the Mullica River (S = 0.0008), t_{cr} = 8.5 \pm 2.2 Pa, similar to the directly measured value of (4.5 \pm ~1 Pa) (Dunne and Jerolmack, 2020), particularly after recognizing that the bankfull shear stress overestimates the shear stress along the banks by ~20% (Parker, 1978).

Although consistent with previous practice (Dade and Friend, 1998; Li et al., 2015; Li et al., 2016), a criticism of Fig. 3 is that it overstates the goodness of fit because of the autocorrelation between the variables on the x- and y-axes, which are both functions of grain size. To avoid this autocorrelation, in Fig. 4 we replot the data as the bankfull shear stress t_{bf} (Fig. 4a) and slope-scaled shear stress t_{bf} / S^{1-a} (Fig. 4b). From Eqs. (1) and (8):

$$\theta_{bf} = \frac{\tau_{bf}}{R\rho_f gd} \tag{12}$$

$$T_{bf}S^{1-\alpha} = \frac{\tau_{bf}}{R\rho_f gd} \tag{13}$$

Substituting these into Eqs. (7) and (10), the models corresponding to Eqs. (7) and (10) are then:

$$\tau_{bf} = R\rho_f g\theta_{cr}(d+d_o) \tag{14}$$

$$\frac{\tau_{bf}}{S^{1-\alpha}} = R\rho_f g T_{cr}(d+d_o) \tag{15}$$

Even in the absence of the autocorrelation in Fig. 3, the above models reasonably represent the trend of the data, especially when the bed shear stress is scaled by slope (Fig. 4b).

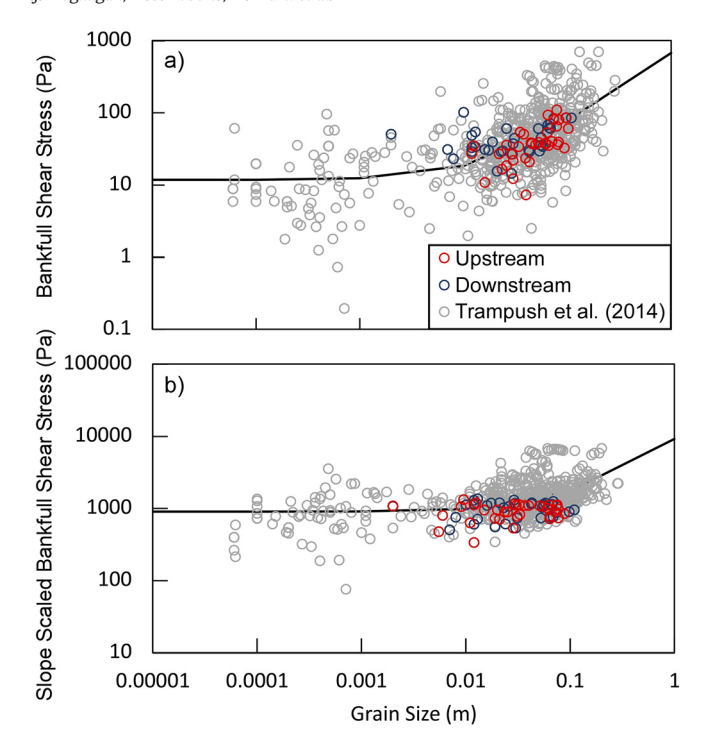


Fig. 4. Bankfull bed shear stress (a) and slope-scaled bed shear stress (b) values as a function of grain size. Solid lines are best fit models representing a linear combination of bedload and suspended load components (Eqs. (14) and (15)). Gray circles show the distribution of bankfull bed shear stress and slope-scaled bed shear stress values compiled by Trampush et al. (2014) taken to represent streams in equilibrium with modern conditions. Bankfull bed shear stress and slope-scaled bed shear stress values upstream (red circles) and downstream (blue circles) are indistinguishable from each other and from those of streams in equilibrium.

Because we assume that the channels in the Trampush et al. (2014) data are representative of the natural variation of channel form for undisturbed systems, we propose that channels in equilibrium have bankfull channel bed shear stresses and Shields values similar to those shown in Figs. 3 and 4. Conversely, bankfull channel shear stresses or Shields values significantly different than those in Figs. 3 and 4 are indications that the channel is in a state of disequilibrium.

3.2. Bedload transport

To monitor bedload transport, 150-171 radio-tagged (Radio Frequency Identification, RFID) bedload sediment tracers (Olinde and Johnson, 2015; Papangelakis and Hassan, 2016; Vazquez-Tarrio et al., 2019) were deployed at cross sections within and upstream of the reservoir at each site (Fig. 5). These tracer rocks ranged in size from 15 to 81 mm (b-axis), similar to the range of median grain sizes measured along transects above and below the RoR dams (8-110 mm). Tracers were fabricated using rocks collected from the study sites or nearby rivers. Two types of half-duplex RFID tag sizes were primarily used (23 and 32 mm), which were supplied by Oregon RFID and provide a read range of ~0.5–0.9 m. Rocks were cut with a rock saw to create a small slit, minimizing the overall reduction in particle mass. RFID tags were implanted in these notches, and glued in using an epoxy sealant. Analysis of slotted particle and uncut rock densities show no significant difference in particle density caused by the incision (Wilcoxon rank-sum test, p = 0.52). All rock b-axes were measured, and the unique tag number of each rock was recorded. Because of the size of the RFID tags, tracer particles measured no smaller than ~23 mm in the largest axis. However, a limited number of particles were fabricated with 12 mm tags; approximately 20 of these particles were deployed at WIND. These smaller tags were not used at other sites because of their limited detection range.

Rocks were deployed in two installments. Between 50 and 80 rocks were placed at each of CBR, FBR, and WAM in summer 2016. Then between 70 and 100 additional tagged clasts were placed at each of these sites in early spring 2017, raising totals at each site to 150–170. WIND was not monitored until spring 2017, when 171 rocks were placed at the site. Rocks were deployed at five cross sections per site over a distance of 150 m to 250 m upstream of the dam. Three of the cross sections were within the reservoir upstream of the dam and two above the reservoir (Fig. 5). Approximately 20–30 tracers were placed at each cross section. Rocks at all sites were placed at approximately regular spacing along cross sections by dropping gently onto the bed at close range. No attempt was made to embed the tracer into the bed. For each site, rocks were organized such that the deployed grain sizes were equally represented at all deployment cross sections. Once deployed, tracers were not removed during the experiment and were left in place after post-deployment detection.

Tracer rock surveys were performed regularly throughout the study period excluding winter months but especially after high-flow events. Survey equipment included a close-range mobile RFID antenna and logger. Channels were surveyed in a zigzag pattern in the downstream direction. Upon rock detection, its identification number and qualitative location were recorded, with reference to a survey landmark (cross section, control point, dam crest, etc.). In spring 2017, survey techniques were enhanced with the use of a Trimble Geo 7× handheld GPS unit to determine tracer rock locations with greater precision (\sim 1-2 m) after post-processing with differential correction. The GPS system was also used to locate each cross section, allowing for the initial location of each tracer to be determined with similar precision. For each tagged clast that moved, we calculated the cumulative total distance moved over the sampling period to quantify virtual velocity. Virtual velocity can be represented in several ways (Vazquez-Tarrio et al., 2019), but because hydrograph or flow data were incomplete, we cannot determine duration of time above an entrainment threshold (c.f., Mao et al., 2017). Thus we define virtual velocity simply as total distance transported over time period deployed, similar to the approach utilized by Beechie (2001).

3.3. Channel Geometry

Eight to fourteen cross sections were established at each dam site, spaced ~20 to 100 m apart. Cross sections were systematically placed depending on measured spacing, regardless of the bed morphology of the channel at that location (e.g., riffles were not preferentially selected). Cross sections were oriented perpendicular to flow and longitudinal profiles through the thalweg were surveyed using a robotic total station. Bankfull width was identified in the field using changes in slope between the channel and floodplain and changes in riparian vegetation. Bankfull depth was determined from the topographic cross section as the average depth at the stage corresponding to the bankfull width. For consistency, slopes were determined over a distance equal to 15 times bankfull channel widths centered at the cross section (Prestegaard, 1983). Median grain size was quantified using Wolman pebble counts (Wolman, 1954) of 100 grains per cross section. All sediment with a b-axis of 2 mm or less was recorded as sand and used to determine the percent sand at each cross section.

4. Results

4.1. Tracer rock surveys

The percentage of tracers recovered varies by site, from just under half of all tracers at the site with the largest drainage area (MAS) to almost all tracers at two with the smallest drainage areas (CBR and FBR) (Table 2). All sites had tracers that did not move (between 10%–29%). Of the 791 total tagged rocks placed at all five sites, 503 tracers were relocated after being transported from their deployment location.

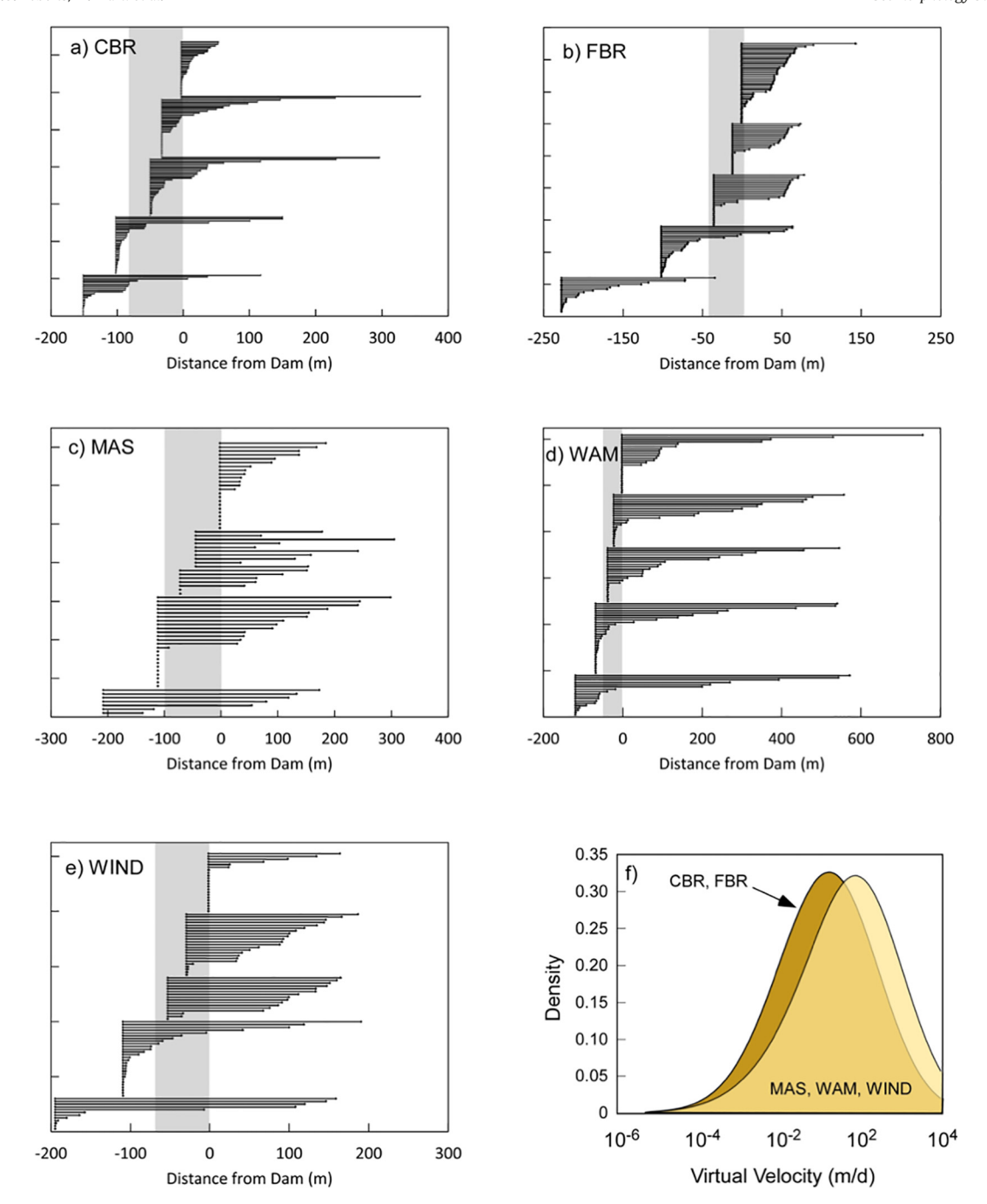


Fig. 5. Tracer rock displacements. Lines indicate initial and final location of each recovered tracer, with flow from left to right. Shaded region indicates reservoir upstream of dam. Gaussian kernel densities for the two groups of sites with similar virtual velocity distributions are shown in the lower right. (Color figure available online)

Table 2Summary of tracer recovery and transport.

Site	Total tracers Percent deployed (year) recovered		Average travel distance of recovered tracers (m)	Percent of recovered tracers that did not move	# tracers over dam	Maximum tracer size tranported over dam	Days in reservoir	
			(Avg. ± SD)			(mm)	Avg. ± SD	
CBR	57 (2016) 150 (2017)	98	44 ± 71	10	50	65	203 ± 146 (n = 44)	
FBR	70 (2016) 170 (2017)	99	42 ± 44	12	79	59	$148 \pm 115 (n = 54)$	
MAS	71 (2016) 150 (2017)	47	123 ± 120	29	46	73	$159 \pm 118 (n = 28)$	
WAM	71 (2016) 150 (2017)	81	139 ± 193	24	56	67	$153 \pm 123 \ (n=41)$	
WIND	171 (2017)	60	79 ± 92	18	45	49	$19 \pm 30 \ (n = 37)$	

Among those tracers that moved and were relocated, the maximum cumulative displacement during the study period by any rock was 758 m, and the median cumulative distance traveled was 30 m. All transects upstream of their respective dams, excluding the most upstream transect of FBR, had tracers that were transported over the dam (Fig. 5), with MAS having the least percentage (21%) of tracers transported over the dam (Table 2). Of the 276 tracers transported over a dam, 204 spent time in the reservoir prior to transmission downstream (i.e., 72 tracers were transported from upstream of the reservoir to below the dam in a single event). Among those tracers that spent time in the reservoir prior to transport over the dam, the average reservoir residence times at the different sites ranged from 19 to 203 days (Table 2). The median grain sizes of rocks that were transported over the dam were identical to those that moved during the study period and similar to the d_{50} of all sampled grains in all the transects. The largest grains transported over the dam at the different sites ranged between 49 and 73 mm.

Of those tracers that moved, the distribution of virtual velocities was close to log-normal and very broadly distributed over more than six orders of magnitude. An analysis of variance (ANOVA) revealed that these virtual velocities collapse into two main distributions (Fig. 5f); CBR and FBR having slower virtual velocities (arithmetic mean of 0.36 and 0.31 m/d (42 and 52 m/yr), respectively) with MAS, WAM, and WIND having higher virtual velocities (arithmetic mean of 1.17, 1.18, and 1.1 m/d (198, 149, and 142 m/yr), respectively). The slower virtual velocities occur along the reaches with higher average slopes (0.028 at both CBR and FBR versus 0.01 or less at MAS, WAM, and WIND). Higher slopes are generally associated with channel morphologies with greater macro roughness (Montgomery and Buffington, 1997). We speculate that this greater roughness may slow the transport of sediment, resulting in slower virtual velocities. The shift to increasing virtual velocity with increasing watershed area corresponds to a similar modeled trend identified by Pizzuto et al. (2014) with their pan-watershed analysis of time-averaged velocities for the silt-clay and sand-sized fractions of suspended load.

4.2. Channel geometry

Fig. 6 compares the average change in the various channel geometry metrics between upstream and downstream transects at each site, with a positive number representing an increase in the downstream reach. No consistent trend was found in any of the channel geometry metrics across the different sites and among the RoR dams only two of the changes are statistically significant; an increase in bankfull depth below WIND (two tailed t-test p=0.04), and an increase in channel slope below CBR (p=0.03). Marginally significant decreases in channel slope occurred below BMD (p=0.07) and WIND (p=0.08). Percent changes in bankfull Shields values among the RoR dams were generally larger than the changes in individual metrics, but neither consistent across sites nor statistically significant. In comparison, significant changes in bankfull depth and slope were observed below the OBD impoundment dam, yet here too no significant change in bankfull Shields values was observed.

That no significant change in bankfull channel geometry occurred below the RoR dams is also shown by the distribution of bankfull Shields values and bed shear stresses above and below the RoR dams shown in Figs. 3 and 4. The distributions of bankfull Shields values and bed shear stresses upstream and downstream of the dams are indistinguishable and both are similar to those of the nominally undisturbed channels compiled by Trampush et al. (2014), suggesting that the channels have developed an equilibrium form despite any potential disturbance caused by the dam.

5. Discussion

Unlike larger flow-regulating dams with higher trapping efficiencies and greater accommodation space to store sediment, these results

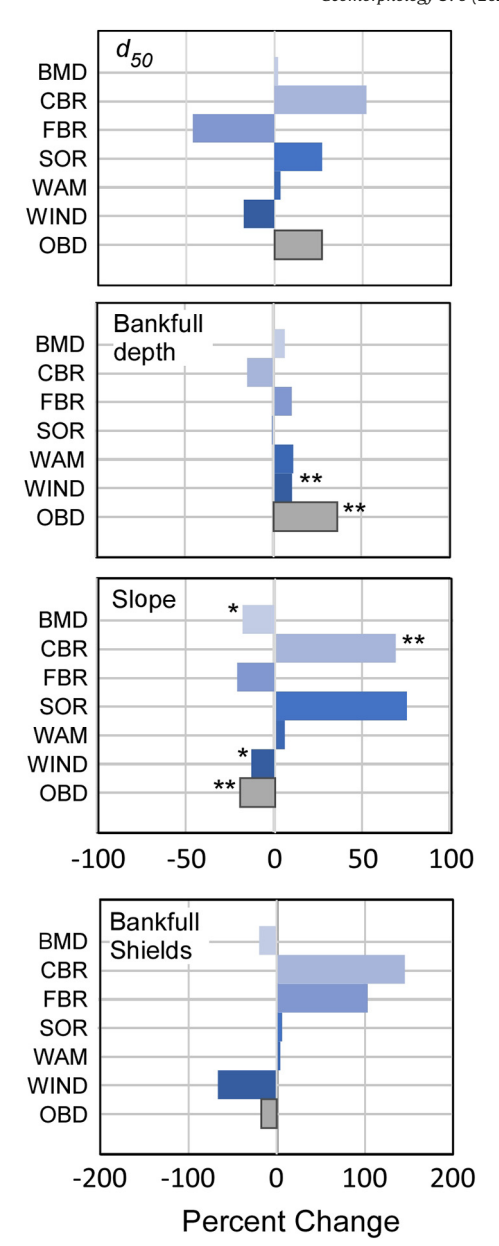


Fig. 6. Percent change in channel geometric metrics at each study site. A positive value represents an increase in the downstream direction. All dams are run of river dams except the OBD impoundment dam. * represents a two tailed t-test p value of <0.1; ** represents a two tailed t-test p value <0.05. (Color figure available online)

demonstrate that RoR dams intermittently permit coarse sediment mobilization into, and out of, their reservoirs, with maximum grain sizes transported over the dam crest exceeding the median grain size of the upstream sediment distributions and as large at 73 mm. Similar to that observed by Pearson and Pizzuto (2015) at a RoR dam in Delaware (USA) and Casserly et al. (2020) in Ireland, the transport of coarse sediment was facilitated by sediment ramps up to near the dam crest (Fig. 7).

For the range of flows occurring during this sampling period – from some of the lowest low flows of the past several decades to a ~5 yr recurrence interval flood – sediment residence times upstream of the RoR dams were less than a year (Table 2). Of the tracers transported over a dam, about one-quarter of the tracers were transported into the reservoir and over the dam in a single high flow event. For the remaining tracers, the reservoir behind the RoR dam acted as a temporary deposition or resting location where, under the right flow conditions, clasts were subsequently re-mobilized out of the reservoir fill.



Fig. 7. (A) Reservoir at WAM. Half of the reservoir behind the dam is dominated by a scour pool over 1 m deep. The other half is dominated by a coarse-bedded sediment ramp that slopes up to the dam. (B) Reservoir just behind the dam at SOR. Sediment is built up on average approximately 40 cm below the dam crest for 100 m behind the dam. (Color figure available online)

By combining RFID tracer particles with existing empirical relations related to bedload transport, Casserly et al. (2020) argued that temporary storage of coarser sediment behind low-head dams, particularly after reservoir scour events, can lead to transient supply-limited conditions downstream that result in lower fractional transport rates below the dam. Supply-limited conditions persist until the reservoir is filled, allowing for the coarse sediment to be transported over the dam. That the reservoir residence times of our tracers were less than a year suggests that any supply-limited conditions at our sites are likely ephemeral.

The construction of the requisite ramp for coarse sediment transport over the RoR dam may take decades or longer, so we are unable to determine when the presumably initially higher trapping efficiency of the RoR shifts to progressively greater sediment mobilization. Regional erosion rates are poorly constrained for New England but generally vary between 2 and 5 mm/kyr (Dethier et al., 2016; Gordon, 1979). For the initial post-dam reservoir capacities at our sites, a drainage area weighted estimate would require ~10–20 yr to attain current volumes of fill, and similar to what Pearson and Pizzuto (2015) document, each dam has existed long enough to have been filled many times over. In essence, for these low head impoundments, the accommodation space of these reservoirs is small compared to the size of their watersheds and to annual sediment discharge.

The short residence times and minimal trapping in the reservoirs indicate that much of the upstream sediment is mobilized downstream. Given this high degree of sediment connectivity, we expect and observe the RoR dams to force few geomorphic adjustments downstream of the dams. Individual channel form metrics downstream of the dams, such as grain size, width, depth or slope, differed in many ways from upstream reaches, but the differences were inconsistent in direction and magnitude within and among the sites and few of the differences were statistically significant. Interestingly, however, despite the changes in individual metrics, downstream reaches have mutually adjusted to generate similar values of the bankfull Shield parameter and bed shear stresses (Figs. 3 and 4) consistent with the nominally undisturbed channel geometries compiled by Trampush et al. (2014). This indicates that the downstream channels have developed equilibrium morphologies despite the intermittent flux of sediment.

Although it is impossible to determine how long it takes to re-establish an equilibrium channel form relative to the initial emplacement of the dam(s), these dams have been in place for >50 yr and the downstream channels are presently adjusted to the generally connected sediment

supply following the construction of the ramp. In many ways, dam removal may provide an approximate proxy for channel adjustments following ramp construction that facilitates sediment flux. In a dam removal in the nearby Amethyst Brook, Magilligan et al. (2016a) documented significant changes in grain size and channel morphology within the first year following removal. These rapid downstream adjustments following dam removal have been documented elsewhere (Foley et al., 2017; Grant and Lewis, 2015; Major et al., 2017; Sawaske and Freyberg, 2012) suggesting that once the ramp in existing RoR dams can sufficiently transmit sediment, downstream channels may respond quickly.

Moreover, despite the presence of the impoundments, the virtual velocities across our sites (Fig. 5f) are strikingly similar to those compiled in Beechie (2001) (Fig. 8). The range in virtual velocities across these impounded sites correspond to the range of virtual velocities in undisturbed sites, once again reinforcing that our sampling sites have generated profiles and channel morphologies in line with" natural" conditions despite the presence of these low head RoR dams.

Where sediment storage is more pronounced, as with OBD, significant geomorphic adjustments occur (Fig. 6). Yet despite the robust

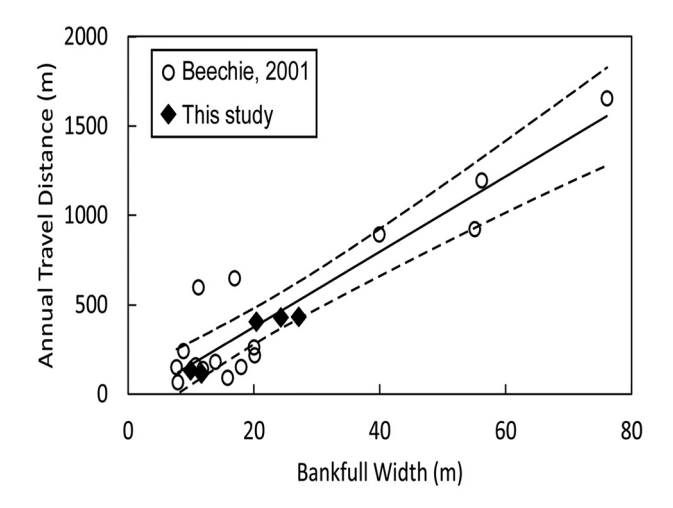


Fig. 8. Annual travel distance of tracers across RoR sites compared to those compiled by Beechie (2001). Dashed lines indicate 95% confidence intervals for linear fit (solid line) to the data from Beechie (2001).

changes in streamflow at OBD where the pre-dam bankfull discharge has never occurred following impoundment (Magilligan et al., 2008), and the enhanced sediment trapping of the larger reservoir, dam proximal reaches have adjusted to attain bankfull Shield values similar to those upstream in the ~60 yr since the dam was constructed (Fig. 6). We focused our response reach to within the first several hundred meters below the dam, so it is not possible to ascertain the longitudinal extent of continued similarity of bankfull Shields values below OBD, but no doubt the effect is spatially limited and would be shifted significantly out of equilibrium when the next major tributary enters (Curtis et al., 2010).

6. Conclusion

For the scale of RoR dams we sampled, our results indicate that over decadal time spans they are similar to natural morphological traps in a river reach like deep pools or large woody debris (LWD) that have limited sediment residence times (Fisher et al., 2010; Lisle and Hilton, 1992). During the study period, which included both low and moderate hydrologic regimes, bedload tracer particles moved through the reservoir on the order of days to weeks. Through the construction of a sediment ramp up to the dam crest (Casserly et al., 2020; Pearson and Pizutto, 2015), RoR dam reservoirs ultimately get configured to transmit and trap the upstream sediment supply within the same range of physical conditions that produce mobility and trapping in the river's natural reach-scale morphological units. Because RoR dams are likely not trapping more sediment than is typically sequestered in natural river reaches, these dams do not generate major anthropogenicallyimposed interruptions to sediment connectivity on a watershed scale nor do they generate morphologic disequilibrium below the dams. However, the minimal effect that small, channel spanning RoR dams have on the equilibrium state of channel form does not suggest that RoR dams do not have an ecological footprint. Their individual and collective presence in a watershed still serves to interrupt ecologic connectivity, such as obstructing fish passage, which can persist regardless of transient sediment connectivity (Hall et al., 2011; Januchowski-Hartley et al., 2013; Neeson et al., 2015; Santucci et al., 2005; Wohl et al., 2019).

Lastly, these results lie very much at the intersection of new, novel approaches for sediment tracing (e.g., RFID PIT tagging), and the application of these technologies in quantifying the potential of low head, run-of-river structures to disconnect watershed sediment flux in a similar fashion as larger flow regulating flood control or hydropower dams that significantly reduce significant water and sediment discharges (Graf, 1999; Magilligan et al., 2013). Recent research in European rivers (Depret et al., 2019; Peeters et al., 2020; Sindelar et al., 2017) indicates that the mobilization of gravel through weirs (analogous to low head RoR structures that we evaluate) can be a common occurrence, although in those European examples, opened or partially breached sluice gates serve to enhance the gravel passage. For the examples we present herein, we show that the progressive development of the gravel ramp up to the dam crest - similar to what Pearson and Pizutto (2015) initially identified – fundamentally enhances sediment mobilization over the dam crest. Our pan-watershed analysis indicates that material coarser than the median can be mobilized over the dam crest under the right conditions similar to what Casserly et al. (2020) observed at their two RoR sites. Importantly, in the geomorphic and structural situations we describe, clasts that get transported from the upstream control section do not get completely sequestered in the reservoir during the step-like transport; i.e., clasts once transported into the low velocity, seemingly lentic reaches of the impoundment can be subsequently mobilized through and beyond the reservoir, sustaining sediment connectivity. These results further indicate that leaving dams in place to prevent stored contaminated sediments from being mobilized downstream may not be a valid argument as the residence time of stored, coarse material is frequently less than a year.

Declaration of competing interest

The authors declare that they have no known competing financial interests or personal relationships that could have appeared to influence the work reported in this paper.

Acknowledgements

This research was supported in part by the National Science Foundation (BCS-1636415), a Dartmouth College Provost Seed Grant, a CompX Grant from Dartmouth's Neukom Institute for Computational Science, and a Geological Society of America Graduate Student Research Grant. We would like to thank Will Shafer, Brad Geismar, Olivia Lantz, and Andrew Crutchfield for help with field work, and both Jonathan Chipman and James Dietrich for geospatial guidance. We greatly appreciate the comments and suggestions by Adam Pearson and the two anonymous reviewers that greatly improved the paper.

References

- Ashley, J.T.F., Bushaw-Newton, K., Wilhelm, M., Boettner, A., Drames, G., Velinsky, D.J., 2006. The effects of small dam removal on the distribution of sedimentary contaminants. Environ. Monit. Assess. 114 (1–3), 287–312.
- Beechie, T.J., 2001. Empirical predictors of annual bed load travel distance, and implications for salmonid habitat restoration and protection. Earth Surf. Process. Landf. 26 (9), 1025–1034.
- Brandt, S.A., 2000. Classification of geomorphological effects downstream of dams. Catena 40 (4), 375–401.
- Brune, G.M., 1953. Trap efficiency of reservoirs. Trans Amer Geophy Union 34 (3), 825–830.
- Casserly, C.M., Turner, J.N., O'Sullivan, J.J., Bruen, M., Bullock, C., Atkinson, S., Kelly-Quinn, M., 2020. Impact of low-head dams on bedload transport rates in coarse-bedded streams. Science of the Total Environment, 716, r.
- Church, M., 1995. Geomorphic response to river flow regulation case-studies and time-scales. Regulated Rivers-Research & Management 11 (1), 3–22.
- Csiki, S.J.C., Rhoads, B.L., 2010. Hydraulic and geomorphological effects of run-of-river dams. Prog. Phys. Geogr. 34, 755–780.
- Csiki, S.J.C., Rhoads, B.L., 2014. Influence of four run-of-river dams on channel morphology and sediment characteristics in Illinois, USA. Geomorphology 206, 215–229.
- Curtis, K.E., Renshaw, C.E., Magilligan, F.J., Dade, W.B., 2010. Temporal and spatial scales of geomorphic adjustments to reduced competency following flow regulation in bedload-dominated systems. Geomorphology 118 (1–2), 105–117.
- Dade, W.B., Friend, P.F., 1998. Grain size, sediment-transport regime and channel slope in alluvial rivers. J. Geol. 106, 661–675.
- Dade, W.B., Renshaw, C.E., Magilligan, F.J., 2011. Sediment transport constraints on river response to regulation. Geomorphology 126 (1–2), 245–251.
- Depret, T., Piegay, H., Dugue, V., Vaudor, L., Faure, J.B., Le Coz, J., Camenen, B., 2019. Estimating and restoring bedload transport through a run-of-river reservoir. Sci. Total Environ. 654. 1146–1157.
- Dethier, E., Magilligan, F.J., Renshaw, C.E., Nislow, K.H., 2016. The role of chronic and episodic disturbances on channel-hillslope coupling: the persistence and legacy of extreme floods. Earth Surf. Process. Landf. 41 (10), 1437–1447.
- Dunne, K.B.J., Jerolmack, D.J., 2020. What sets river width? Sci. Adv., 6(41), eabc1505.
- Dunne, K.B.J., Arratia, P., Jerolmack, D.J., 2019. A New Method for In-situ Measurement of the Erosion Threshold of River Channels (EarthArXiv).
- Fencl, J.S., Mather, M.E., Costigan, K.H., Daniels, M.D., 2015. How big of an effect do small dams have? Using geomorphological footprints to quantify spatial impact of low-head dams and identify patterns of across-dam variation. PLoS One 10 (11).
- Fisher, G.B., Magilligan, F.J., Kaste, J.M., Nislow, K.H., 2010. Constraining the timescales of sediment sequestration associated with large woody debris using cosmogenic Be-7. Journal of Geophysical Research-Earth Surface, 115.
- Foley, M.M., Bellmore, J.R., O'Connor, J.E., Duda, J.J., East, A.E., Grant, G.E., Anderson, C.W., Bountry, J.A., Collins, M.J., Connolly, P.J., Craig, L.S., Evans, J.E., Greene, S.L., Magilligan, F.J., Magirl, C.S., Major, J.J., Pess, G.R., Randle, T.J., Shafroth, P.B., Torgersen, C.E., Tullos, D., Wilcox, A.C., 2017. Dam removal: Listening in. Water Resour. Res. 53 (7), 5229–5246
- Gordon, R.B., 1979. Denudation rate of central New England determined from estuarine sedimentation. Am. J. Sci. 279 (6), 632–642.
- Graf, W.L., 1999. Dam nation: a geographic census of American dams and their large-scale hydrologic impacts. Water Resour. Res. 35 (4), 1305–1311.
- Grant, G.E., Lewis, S.L., 2015. The remains of the dam: what have we learned from 15 years of US dam removals? In: Lollino, G., Arattano, M., Rinaldi, M., Giustolisi, O., Marechal, J.-C., Grant, G.E. (Eds.), Engineering Geology for Society and Territory Volume 3. Springer, New York, pp. 31–33
- Gregory, K.J., Park, C., 1974. Adjustment of river channel capacity downstream from a reservoir. Water Resour. Res. 10 (4), 870–873.
- Hall, C.J., Jordaan, A., Frisk, M.G., 2011. The historic influence of dams on diadromous fish habitat with a focus on river herring and hydrologic longitudinal connectivity. Landsc. Ecol. 26 (1), 95–107.

- Januchowski-Hartley, S.R., McIntyre, P.B., Diebel, M., Doran, P.J., Infante, D.M., Joseph, C., Allan, J.D., 2013. Restoring aquatic ecosystem connectivity requires expanding inventories of both dams and road crossings. Front. Ecol. Environ. 11 (4), 211–217.
- Tories of both dams and road crossings. Front. Ecol. Environ. 11 (4), 211–217. Juracek, K.E., 2000. Channel stability downstream from a dam assessed using aerial photographs and stream-gage information. J. Am. Water Resour. Assoc. 36 (3), 633–645.
- Kellerhalls, R., 1967. Stable channels with gravel-paved beds. J of the Waterways and Harbors Division 93 (1), 63–84.
- Lamb, M.P., Dietrich, W.E., Venditti, J.G., 2008. Is the critical Shields stress for incipient sediment motion dependent on channel-bed slope? Journal of Geophysical Research-Earth Surface 113 (F2), 1–20.
- Leopold, L.B., Wolman, G.M., Miller, J.P., 1964. Fluvial Processes in Geomorphology. W.H. Freeman, San Francisco.
- Li, C., Czapiga, M.J., Eke, E.C., Viparelli, E., Parker, G., 2015. Variable Shields number model for river bankfull geometry: bankfull shear velocity is viscosity-dependent but grain size-independent. J. Hydraul. Res. 53 (1), 36–48.
- Li, C., Czapiga, M.J., Eke, E.C., Viparelli, E., Parker, G., 2016. Closure to "Variable Shields number model for river bankfull geometry: bankfull shear velocity is viscosity-dependent but grain size-independent". J. Hydraul. Res. 54 (2), 234–237.
- Lisle, T.E., Hilton, S., 1992. The volume of fine sediment in pools an index of sediment supply in gravel-bed streams. Water Resour. Bull. 28 (2), 371–383.
- Mackin, J.H., 1948. Concept of the graded river. Geol. Soc. Am. Bull. 59 (5), 463-511.
- Magilligan, F.J., Haynie, H.J., Nislow, K.H., 2008. Channel adjustments to dams in the Connecticut River Basin: Implications for forested mesic watersheds. Ann. Assoc. Am. Geogr. 98 (2), 267–284.
- Magilligan, F.J., Nislow, K.H., Renshaw, C.E., 2013. Flow regulation by dams. Treatise on Geomophology 9, 794–808.
- Magilligan, F.J., Nislow, K.H., Kynard, B.E., Hackman, A.M., 2016a. Immediate changes in stream channel geomorphology, aquatic habitat, and fish assemblages following dam removal in a small upland catchment. Geomorphology 252, 158–170.
- Magilligan, F.J., Graber, B.E., Nislow, K.H., chipman, J.W., Sneddon, C.S., Fox, C.A., 2016b. River restoration by dam removal: Enhancing connectivity at watershed scales. Elementa: Science of the Anthropocene, doi/10.12952/journal.elementa.000108.
- Major, J.J., O'Connor, J.E., Podolak, C.J., Keith, M.K., Grant, G.E., Spicer, K.R., Pittman, S., Bragg, H.M., Wallick, J.R., Tanner, D.Q., Rhode, A., Wilcock, P.R., 2012. Geomorphic response of the Sandy River, Oregon, to removal of the Marmot Dam. U.S. Geol. Surv. Prof. Pap. 1792, 1–64.
- Major, J.J., East, A.E., O'Connor, J.E., Grant, G.E., Wilcox, A.C., Magirl, C.S., Colins, M.J., Tullos, D.D., 2017. Geomorphic responses to dam removal in the United States a two-decade perspective. In: Tsutsumi, D., Laronne, J.B. (Eds.), Gravel-Bed Rivers. John Wiley & Sons, New York.
- Mao, L., Picco, L., Lenzi, M.A., Surian, N., 2017. Bed material transport estimate in large gravel-bed rivers using the virtual velocity approach. Earth Surf. Process. Landf. 42 (4) 595–611
- Montgomery, D.R., Buffington, J.M., 1997. Channel-reach morphology in mountain drainage basins. Geol. Soc. Am. Bull. 109, 596–611.
- Neeson, T.M., Ferris, M.C., Diebel, M.W., Doran, P.J., O'Hanley, J.R., McIntyre, P.B., 2015. Enhancing ecosystem restoration efficiency through spatial and temporal coordination. Proc. Natl. Acad. Sci. U. S. A. 112 (19), 6236–6241.
- Nicholson, S.W., Dicken, C.L., Horton, J.D., Foose, M.P., Mueller, J.A.L., Hon, R., 2006. Preliminary Integrated Geologic Map Databases for the United States: Connecticut, Maine, Massachusetts, New Hampshire, New Jersey, Rhode Island and Vermont. 2006–1272.
- Nilsson, C., Svedmark, M., 2002. Basic principles and ecological consequences of changing water regimes: Riparian plant communities. Environ. Manag. 30 (4), 468–480.
- Nilsson, C., Reidy, C.A., Dynesius, M., Revenga, C., 2005. Fragmentation and flow regulation of the world's large river systems. Science 308 (5720), 405–408.
- NOAA, 2017. National Centers for Environmental Information, State of the Climate: National Climate Report for Annual 2016 (National Oceanic and Atmospheric Administration).
- Olinde, L., Johnson, J.P.L., 2015. Hload transport, step lengths, and rest times in a mountain stream. Water Resour. Res. 51 (9), 7572–7589.
- Papangelakis, E., Hassan, M.A., 2016. The role of channel morphology on the mobility and dispersion of bed sediment in a small gravel-bed stream. Earth Surf. Process. Landf. 41 (15), 2191–2206.

- Parker, G., 1978. Self-formed straight rivers with equilibrium banks and mobile bed 2. Gravel river. Journal of Fluid Mechanics, 89(NOV), 127-&.
- Parker, G., Wilcock, P.R., Paola, C., Dietrich, W.E., Pitlick, J., 2007. Physical basis for quasiuniversal relations describing bankfull hydraulic geometry of single-thread gravel bed rivers. Journal of Geophysical Research-Earth Surface 112 (F4).
- Pearson, A.J., Pizutto, J., 2015. Bedload Transport over Run-of-river Dams, Delaware. U.S.A, Geomorphology.
- Pearson, A.J., Snyder, N.P., Collins, M.J., 2011. Rates and processes of channel response to dam removal with a sand-filled impoundment. Water Resources Research, 47.
- Peeters, A., Houbrechts, G., Hallot, E., Van Campenhout, J., Gob, F., Petit, F., 2020. Can coarse bedload pass through weirs? Geomorphology 359.
- Pizzuto, J., Schenk, E.R., Hupp, C.R., Gellis, A., Noe, G., Williamson, E., Karwan, D.L., O'Neal, M., Marquard, J., Aalto, R., Newbold, D., 2014. Characteristic length scales and time-averaged transport velocities of suspended sediment in the mid-Atlantic Region. USA: Water Resources Research 50, 790–805.
- Poff, N.L., Hart, D.D., 2002. How dams vary and why it matters for the emerging science of dam removal. Bioscience 52 (8), 659–668.
- Prestegaard, K.L., 1983. Variables influencing water-surface slopes in gravel-bed streams at bankfull stage. Geol. Soc. Am. Bull. 94 (5), 673–678.
- PRISM Climate Group, 2004. 30-yr Normal Annual Precipitation 1981–2010. Oregon State University.
- Rainwater, F.H., 1962. Stream Composition of the Coterminous United States. Hydrologic Atlas. U.S, Geological Survey, Washington, D.C.
- Renshaw, C.E., Magilligan, F.J., Doyle, H.G., Dethier, E.N., Kantack, K.M., 2019. Rapid response of New England (USA) rivers to shifting boundary conditions: Processes, time frames, and pathways to post-flood channel equilibrium. Geology 47 (10),
- Roberts, M.O., Renshaw, C.E., Magilligan, F.J., Dade, W.B., 2020. Field measurement of the probability of coarse-grained sediment entrainment in natural rivers. J. Hydraulic Eng., 146(4), 04020024c.
- Santucci, V.J., Gephard, S.R., Pescitelli, S.M., 2005. Effects of multiple low-head dams on fish, macroinvertebrates, habitat, and water quality in the fox river, Illinois. N. Am. J. Fish Manag. 25 (3), 975–992.
- Sawaske, S.R., Freyberg, D.L., 2012. A comparison of past small dam removals in highly sediment-impacted systems in the U.S. Geomorphology 151, 50–58.
- Schumm, S.A., 1960. The shape of alluvial channels in relation to sediment type. USGS Prof. Paper, 352- B(1-30).
- Sindelar, C., Schobesberger, J., Habersack, H., 2017. Effects of weir height and reservoir widening on sediment continuity at run-of-river hydropower plants in gravel bed rivers. Geomorphology 291, 106–115.
- Skalak, K., Pizzuto, J., Hart, D.D., 2009. Influence of small dams on downstream channel characteristics in Pennsylvania and Maryland: implications for the long-term geomorphic effects of dam removal. J. Am. Water Resour. Assoc. 45 (1), 97–109.
- Smith, S.V., Renwick, W.H., Bartley, J.D., Buddemeier, R.W., 2002. Distribution and significance of small, artificial water bodies across the United States landscape. Sci. Total Environ. 299 (1–3), 21–36.
- Syvitski, J.P.M., Vorosmarty, C.J., Kettner, A.J., Green, P., 2005. Impact of humans on the flux of terrestrial sediment to the global coastal ocean. Science 308 (5720), 376–380.
- Trampush, S.M., Huzurbazar, S., McElroy, B., 2014. Empirical assessment of theory for bankfull characteristics of alluvial channels. Water Resour. Res. 50 (12), 9211–9220.
- Vazquez-Tarrio, D., Recking, A., Liebault, F., Tal, M., Menendez-Duarte, R., 2019. Particle transport in gravel-bed rivers: Revisiting passive tracer data. Earth Surf. Process. Landf. 44 (1), 112–128.
- Vorosmarty, C.J., Meybeck, M., Fekete, B., Sharma, K., Green, P., Syvitski, J.P.M., 2003. Anthropogenic sediment retention: major global impact from registered river impoundments. Glob. Planet. Chang. 39 (1–2), 169–190.
- Wohl, E., Brierley, G., Cadol, D., Coulthard, T.J., Covino, T., Fryirs, K.A., Grant, G., Hilton, R.G., Lane, S.N., Magilligan, F.J., Meitzen, K.M., Passalacqua, P., Poeppl, R.E., Rathburn, S.L., Sklar, L.S., 2019. Connectivity as an emergent property of geomorphic systems. Earth Surf. Process. Landf. 44 (1), 4–26.
- Wolman, M.G., 1954. A method of sampling coarse river-bed material. Trans Amer Geophy Union 35 (6), 951–956.